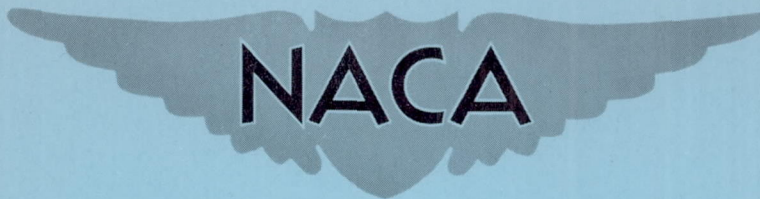


FILE COPY
NO. 5



RM L51A16

NACA RM L51A16



RESEARCH MEMORANDUM

A COMPARISON OF TWO TECHNIQUES UTILIZING ROCKET-PROPELLED
VEHICLES FOR THE DETERMINATION OF THE
DAMPING-IN-ROLL DERIVATIVE

By David G. Stone and Carl A. Sandahl

Langley Aeronautical Laboratory
Langley Field, Va.

THIS DOCUMENT ON LOAN FROM THE FILES OF

NATIONAL ADVISORY COMMITTEE FOR AERONAUTICS
LANGLEY AERONAUTICAL LABORATORY
LANGLEY FIELD, HAMPTON, VIRGINIA

RETURN TO THE ABOVE ADDRESS.

REQUESTS FOR PUBLICATIONS SHOULD BE ADDRESSED
AS FOLLOWS:

NATIONAL ADVISORY COMMITTEE FOR AERONAUTICS
1512 H STREET, N. W.
WASHINGTON 25, D. C.

NATIONAL ADVISORY COMMITTEE FOR AERONAUTICS

WASHINGTON

May 3, 1951

NATIONAL ADVISORY COMMITTEE FOR AERONAUTICS

RESEARCH MEMORANDUM

A COMPARISON OF TWO TECHNIQUES UTILIZING ROCKET-PROPELLED
VEHICLES FOR THE DETERMINATION OF THE
DAMPING-IN-ROLL DERIVATIVE

By David G. Stone and Carl A. Sandahl

SUMMARY

Rocket-powered flight investigations have been conducted for the purpose of comparing damping-in-roll results as obtained from a torque-nozzle technique in which the test configuration is the complete vehicle, and the sting-mount technique in which the test configuration is mounted on a nose sting on the rocket-powered vehicle. The Mach number range of these tests was approximately 0.6 to 1.4 corresponding to Reynolds number ranges of about 1×10^6 to 2.2×10^6 for the sting-mount technique, and about 2.3×10^6 to 8.0×10^6 for the torque-nozzle technique. Good agreement of the damping-in-roll derivative was obtained between the two techniques for a configuration consisting of a pointed cylindrical body having three rectangular unswept wings of NACA 65A009 airfoil sections.

INTRODUCTION

The Pilotless Aircraft Research Division of the Langley Aeronautical Laboratory employs two free-flight techniques for the measurement of the damping-in-roll derivative. In one of these techniques the configuration to be tested is attached to the nose of the rocket vehicle by a sting. The entire test vehicle is forced to roll by offset stabilizing fins. The resulting damping moment of the test configuration is measured by a balance in the nose of the test vehicle. In this sting-mount technique, the models are necessarily small. In the other technique, the test configuration, which is the complete vehicle, is forced to roll by the action of a special rocket nozzle which produces a known torque about the roll axis in addition to thrust during the sustainer rocket burning period. The damping-in-roll derivative is calculated from the measured increment in rolling velocity at a given Mach number between powered and coasting flight.

In order to provide comparative results from the aforementioned techniques, a configuration consisting of a pointed cylindrical body having three rectangular wings employing NACA 65A009 airfoil sections attached near the base of the body was tested by both techniques. The use of a larger model for the torque-nozzle technique and a scale model for the sting-mount technique gave results at widely different Reynolds numbers for comparison and evaluation purposes. The comparisons are made over a Mach number range from about 0.6 to 1.4. The corresponding Reynolds number range was from about 1×10^6 to 2.2×10^6 for the sting-mount technique and from about 2.3×10^6 to 8.0×10^6 for the torque-nozzle technique. The flight tests were conducted at the Pilotless Aircraft Research Station at Wallops Island, Va.

SYMBOLS

C_{l_p}	damping-in-roll derivative	$\left(\frac{\Delta C_l}{\frac{\Delta p b}{2V}} \right)$
C_l	rolling-moment coefficient	$\left(\frac{\text{Rolling moment}}{qSb} \right)$
$pb/2V$	wing-tip helix angle, radians	
q	dynamic pressure, pounds per square foot	
S	total area of three wing panels obtained by extending leading and trailing edges to center line of test vehicle	
b	diameter of circle swept by wing tips, feet	
p	rolling angular velocity, radians per second	
V	flight-path velocity, feet per second	
M	Mach number	

TEST VEHICLES AND TESTS

In both of the techniques compared herein, the damping-in-roll derivatives were obtained only at zero net lift.

Torque-Nozzle Technique

The general arrangement of the configuration tested by means of the torque-nozzle technique is shown in figures 1 and 2. The fuselage, rocket motor, and torque-nozzle arrangement were identical to models described in reference 1. The wing has an aspect ratio of 3.7, no sweep or taper, and NACA 65A009 airfoil sections parallel to the model center line. The wing construction which was used to obtain light but rigid wings is shown in figure 2.

In this technique the test configuration is forced to roll by the action of a special canted rocket nozzle assembly (fig. 2) which produces a known torque about the roll axis in addition to thrust during the rocket burning period. The damping-in-roll derivative is calculated from the increment in rolling velocity at a given Mach number between sustainer-on and coasting flight. It will be noted that in this technique it is unnecessary to correct for any effects of asymmetry of the test wings. This technique is more completely described in reference 1.

Sting-Mount Technique

The general arrangement of the sting-mounted model and the rocket vehicle is shown in figures 3 and 4. The sting-mounted test configuration was a 0.294-scale model of the configuration employed in the torque-nozzle technique.

In this technique the entire test vehicle is forced to roll during flight by the offset stabilizing tail fins. The resulting damping moment of the test configuration is measured by means of a balance in the nose of the test vehicle. The values of C_{l_p} are calculated from this measured moment, after applying corrections for any measured asymmetry of the test wings, assuming that the rolling moment on the test configuration would be zero when the rolling velocity was zero. A description of this sting-mount technique is given in reference 2.

The variation of Reynolds number, based on wing chord, is shown in figure 5 for both techniques. The Reynolds numbers differ by a factor of 3 or greater over the Mach number range.

RESULTS AND DISCUSSION

The basic aerodynamic quantities measured by the two techniques are shown in figure 6. Figure 6(a) illustrates data from the sting-mount technique by showing the helix angles of the vehicle ($pb/2V$ based on the span of the sting-mounted model) produced by the offset stabilizing

fins at the rear. The damping-in-roll derivative C_{l_p} was obtained by dividing the C_l by the $pb/2V$ which assumes that $C_l = 0$ at zero rolling velocity and that C_l is linear with $pb/2V$.

Figure 6(b) illustrates the data from torque-nozzle technique showing the variation of rolling velocity for the known torque or rolling moment produced by the canted nozzles. Shown are the results for two nominally identical models differing only in booster rocket motors so that the resulting Mach number ranges of the data are different but overlapping. The damping-in-roll derivative C_{l_p} was obtained from the known rolling-moment coefficient and the differences in helix angle $\Delta \frac{pb}{2V}$ at a given Mach number as explained more fully in reference 1.

Also shown in figure 6(b) is the wing-dropping phenomenon, reported in reference 3, as evidenced by the abrupt change in $pb/2V$ near $M = 0.9$ in the coasting part of the flight. Shown is a faired line across this wing-drop discontinuity. This fairing is comparable to the assumption that $C_l = 0$ at $\frac{pb}{2V} = 0$ in the sting-mount technique. The discontinuity which occurs in the sustainer-on curves at approximately the same Mach number was not faired out inasmuch as this discontinuity probably reflects some change in the damping in roll as well as a wing-dropping tendency. The $\Delta \frac{pb}{2V}$ values obtained by the fairing across the trim change which occurred during coasting flight were used in determining the C_{l_p} values which are compared with the C_{l_p} values determined from the sting-mount technique in figure 7. The single curve for the torque-nozzle technique was obtained by averaging results obtained with two models employing different boosters.

The comparison of the C_{l_p} values from the two techniques (fig. 7) shows good agreement, even though the Reynolds numbers differed considerably for the two test techniques. Both techniques recorded abrupt changes in the damping in roll in the Mach number range from 0.9 to 1.0 which are not necessarily changes in C_{l_p} , but may result from changes in measured rolling moment or rolling velocity caused by local shock and boundary-layer interaction effects in this Mach number region. The measurement of the damping in roll at transonic speeds of wings which exhibit wing dropping by means of the present techniques, both of which assume that C_{l_p} is constant at a given Mach number, is only qualitative inasmuch as wing dropping may be regarded as resulting in variable C_{l_p} at a given Mach number. It should be noted, however, that the transonic

lateral flying qualities of airplanes having wings susceptible to wing dropping will probably be more affected by this wing dropping than by any damping-in-roll which may be developed.

With the torque-nozzle technique, the effects of variation of helix angle on damping were determined for a range of helix angles from 0.006 to 0.045 radian by the use of different cant angles in the nozzle assemblies (fig. 2) to vary the incremental rolling velocity between sustainer-on and coasting flight. Three cant angles were employed and the results obtained are shown in figure 8. A model with 25° cant angles gave $\frac{\Delta p_b}{2V}$ values of 0.006 to 0.020; two models with 30° cant angles gave $\frac{\Delta p_b}{2V}$ values of 0.008 to 0.032; and two models with 40° cant angles gave $\frac{\Delta p_b}{2V}$ values of 0.011 to 0.045. An average curve is presented for the two models in each case. The ranges of $\frac{\Delta p_b}{2V}$ are such that, in each case, the smaller values of $\frac{\Delta p_b}{2V}$ occurred at the highest Mach numbers and conversely the larger values of $\frac{\Delta p_b}{2V}$ occurred at the lowest Mach numbers. As can be noted in figure 8, for the ranges of helix angles investigated, no significant changes occurred in the damping in roll.

CONCLUSIONS

Comparative damping-in-roll tests of a configuration consisting of a pointed cylindrical body having three rectangular wings of aspect ratio 3.7, no sweep, and NACA 65A009 airfoil sections were made by the torque-nozzle technique and the sting-mount technique. Good agreement between the values of C_{l_p} (damping-in-roll derivative) was obtained in the Mach number range from 0.6 to 1.4 for Reynolds number ranges of 1.0×10^6 to 2.2×10^6 for the sting-mount technique and 2.3×10^6 to 8.0×10^6 for the torque-nozzle technique.

Langley Aeronautical Laboratory
National Advisory Committee for Aeronautics
Langley Field, Va.

REFERENCES

1. Edmondson, James L., and Sanders, E. Claude, Jr.: A Free-Flight Technique for Measuring Damping in Roll by Use of Rocket-Powered Models and Some Initial Results for Rectangular Wings. NACA RM L9I01, 1949.
2. Bland, William M., Jr., and Sandahl, Carl A.: A Technique Utilizing Rocket-Propelled Test Vehicles for the Measurement of the Damping in Roll of Sting-Mounted Models and Some Initial Results for Delta and Unswept Tapered Wings. NACA RM L50D24, 1950.
3. Stone, David G.: Wing-Dropping Characteristics of Some Straight and Swept Wings at Transonic Speeds as Determined with Rocket-Powered Models. NACA RM L50C01, 1950.

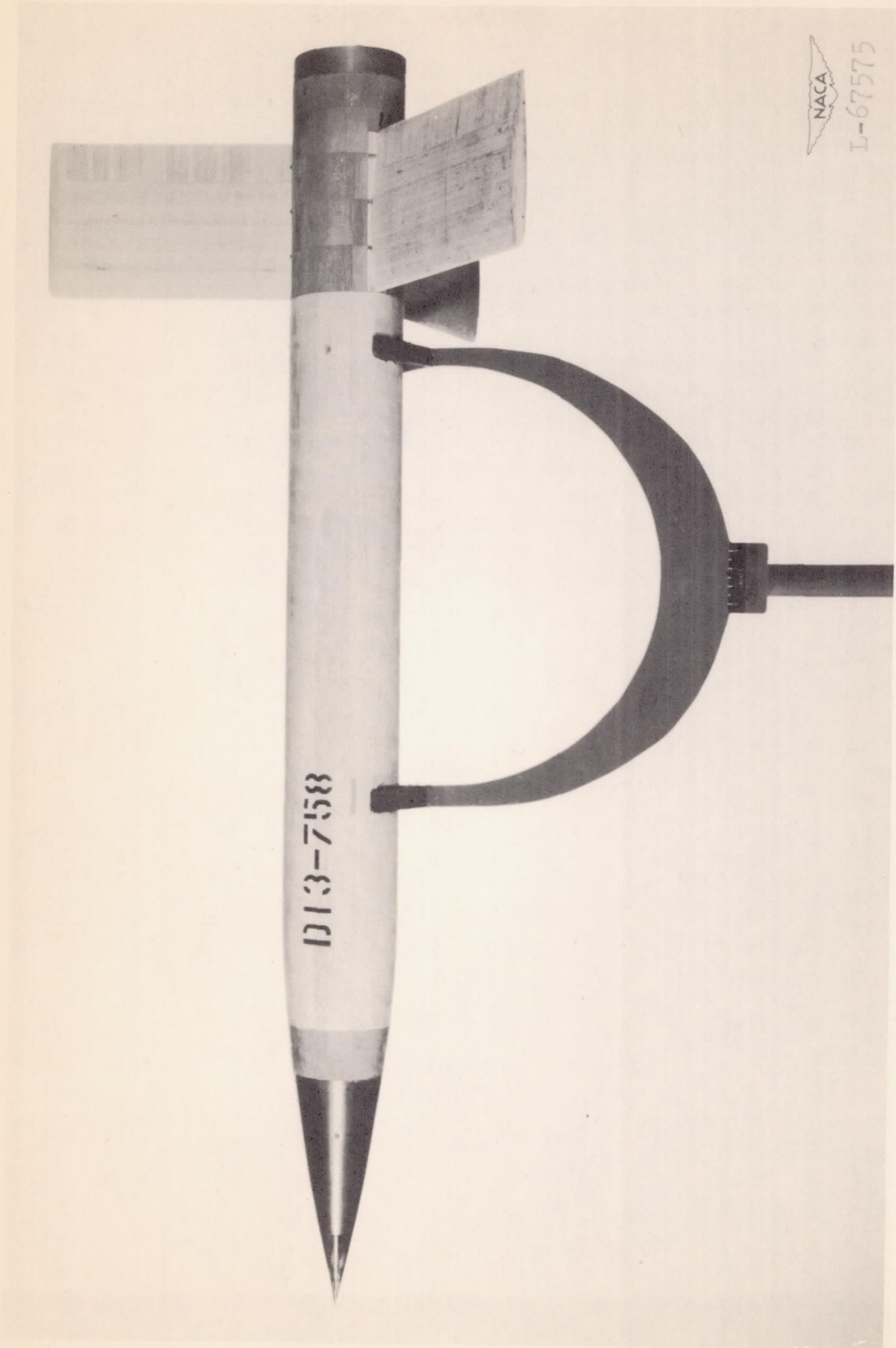
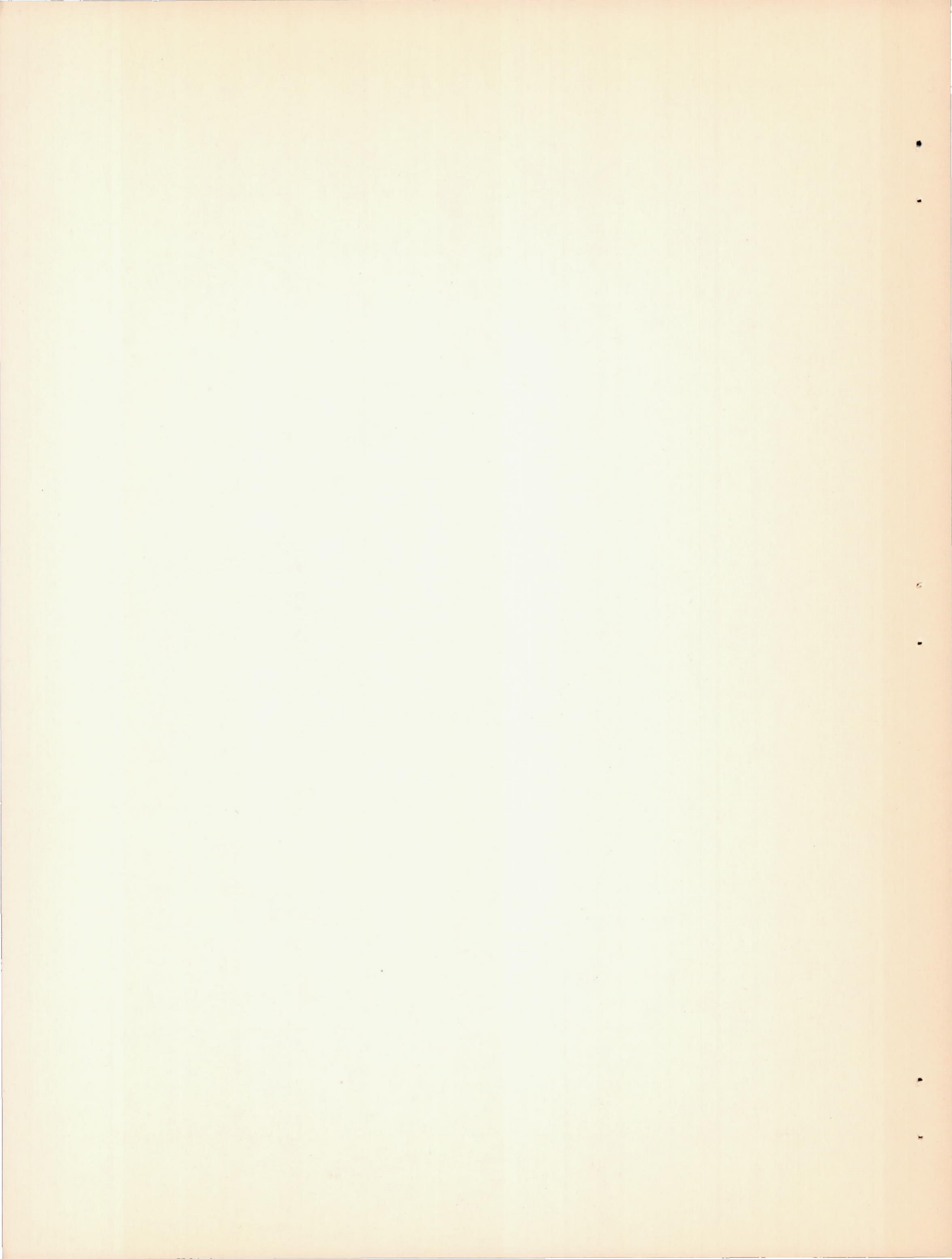
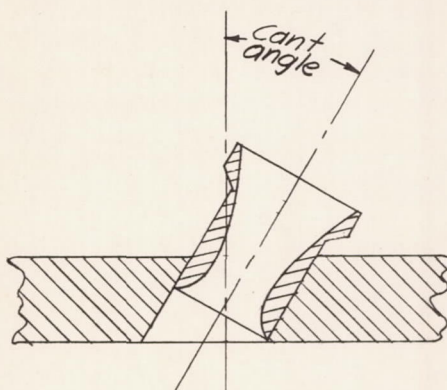
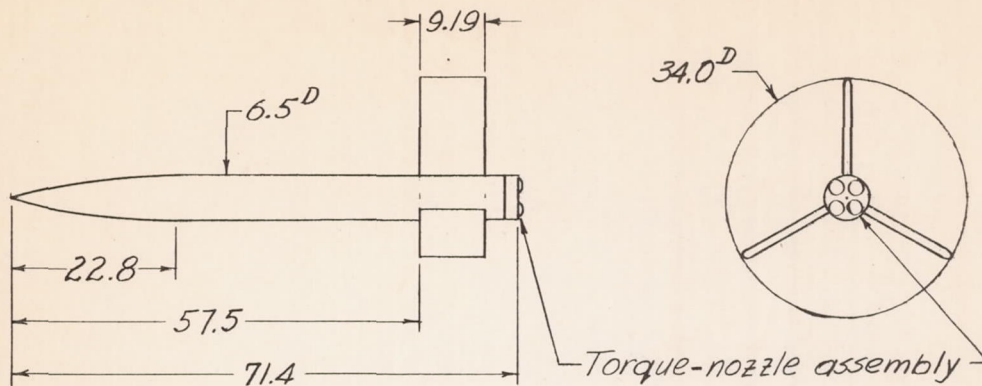
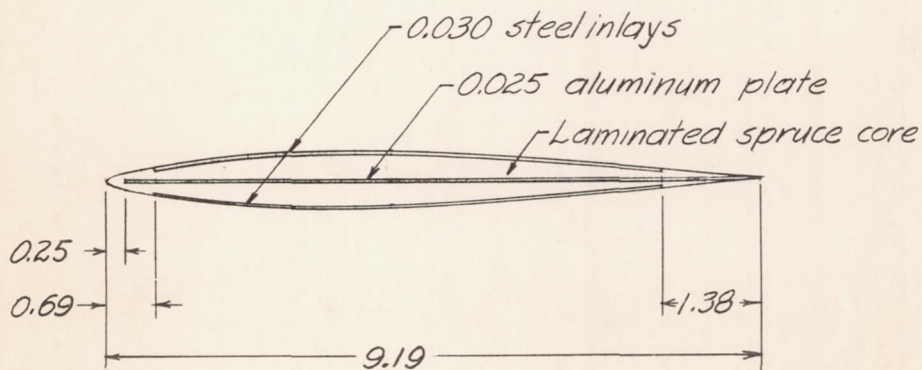


Figure 1.- Torque-nozzle technique configuration.





Detail of individual torque nozzle



Typical airfoil section

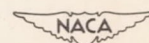
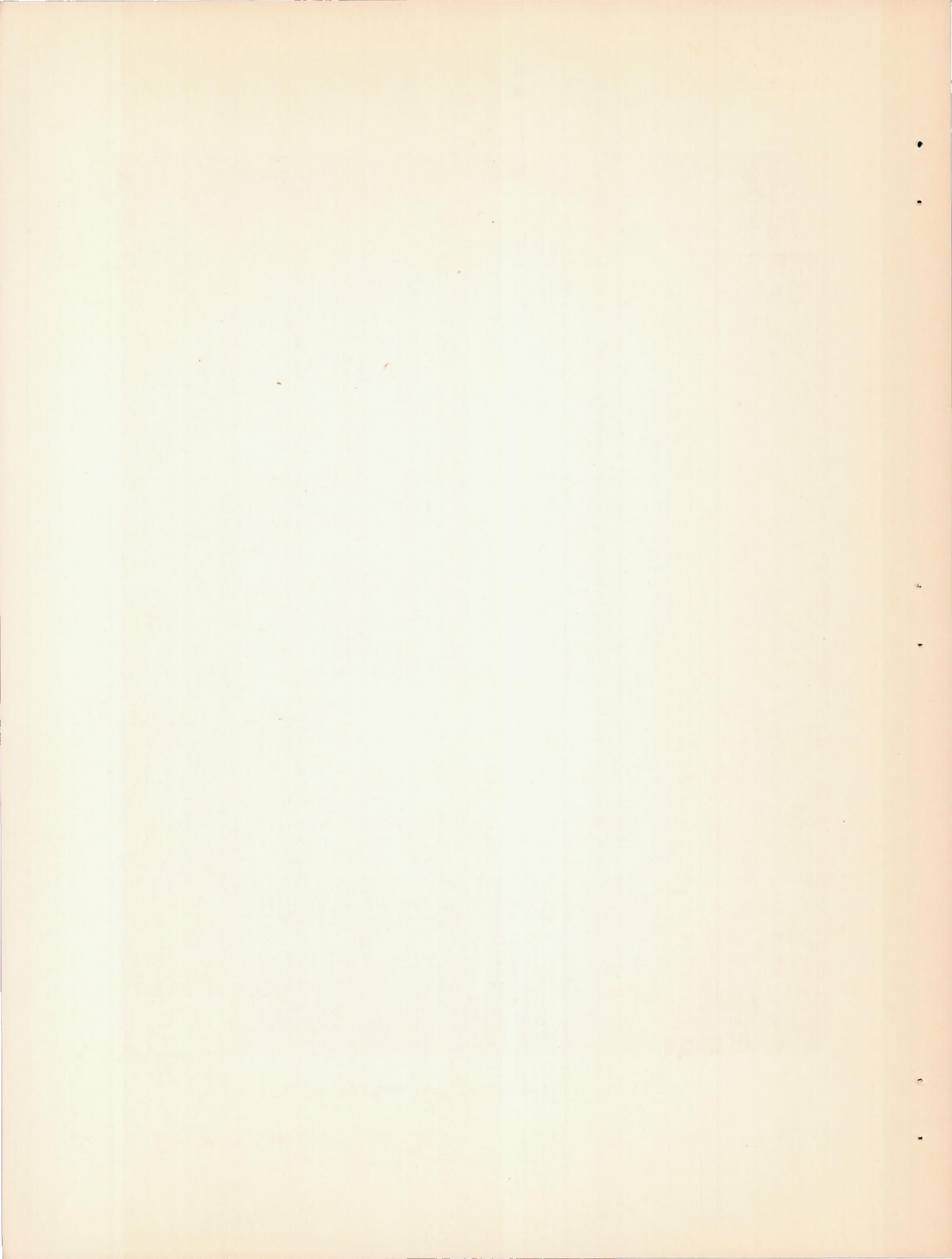


Figure 2.- General arrangement of torque-nozzle configuration. Dimensions are in inches.



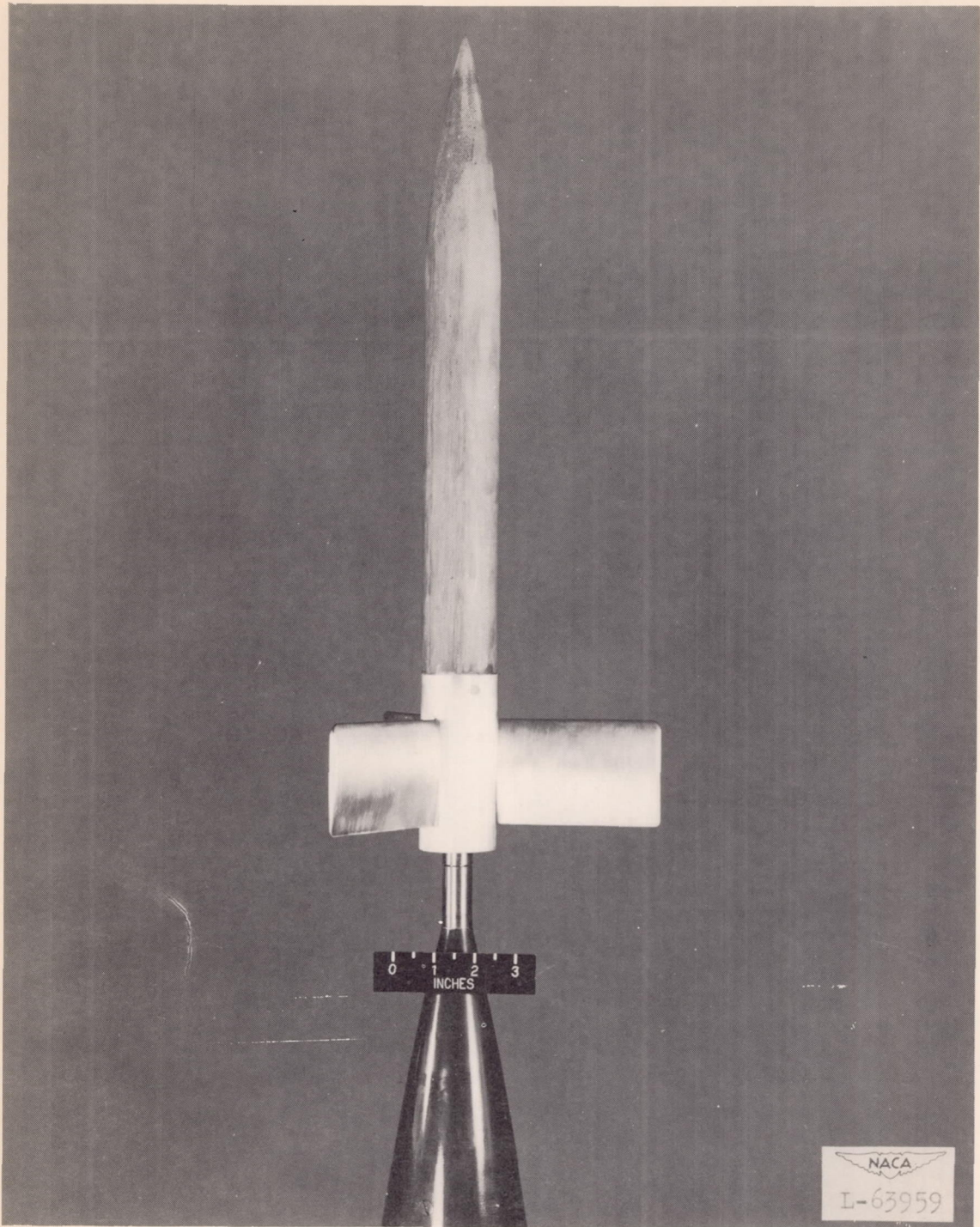
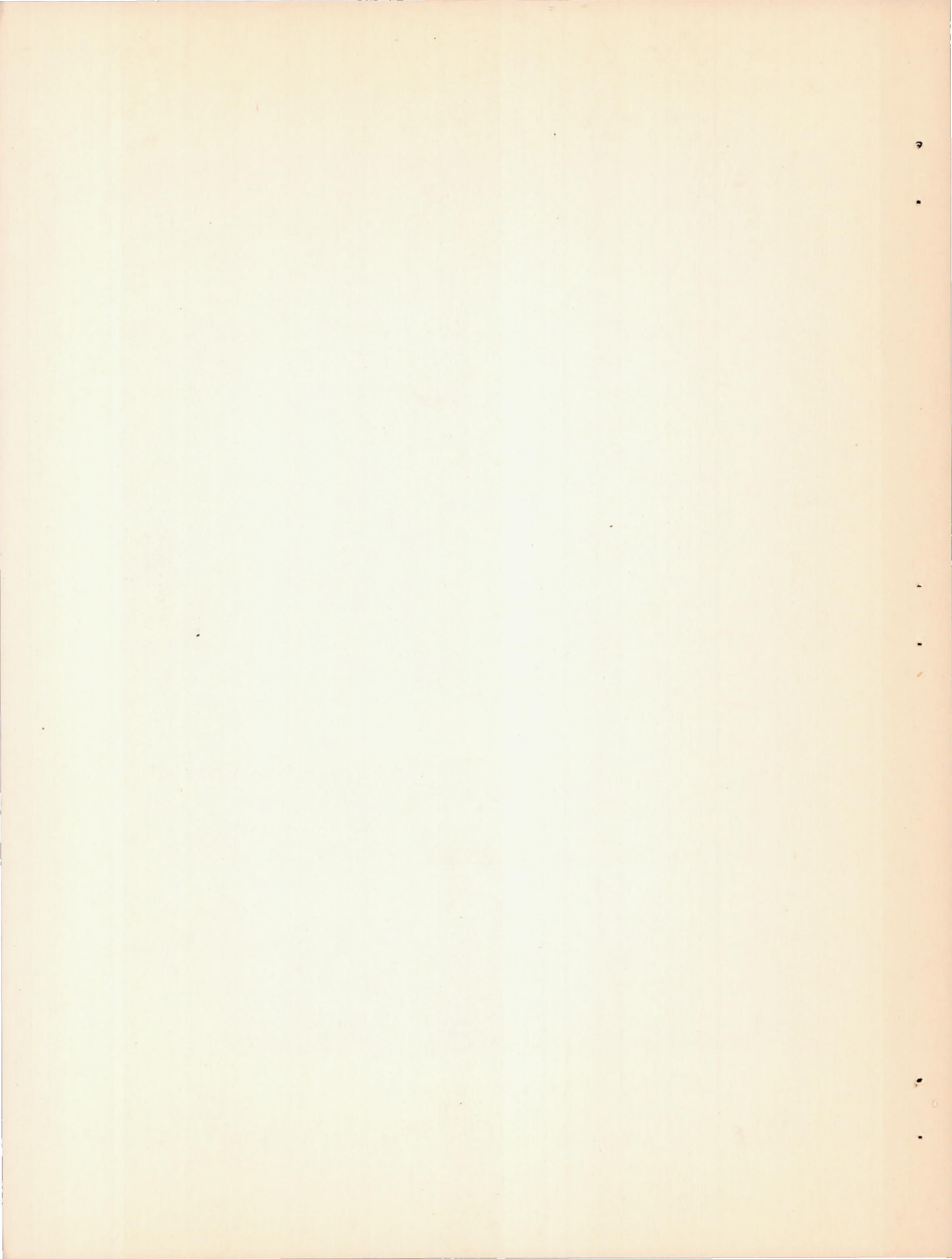
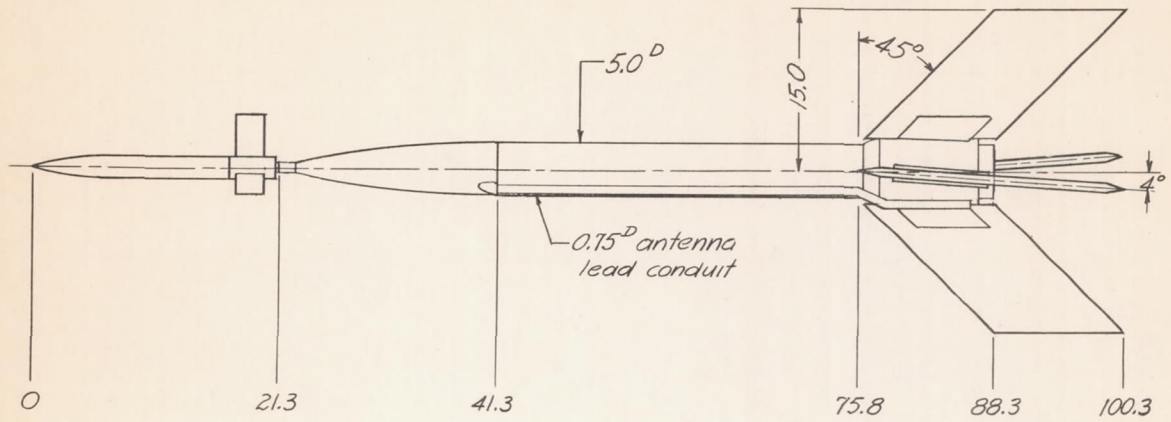
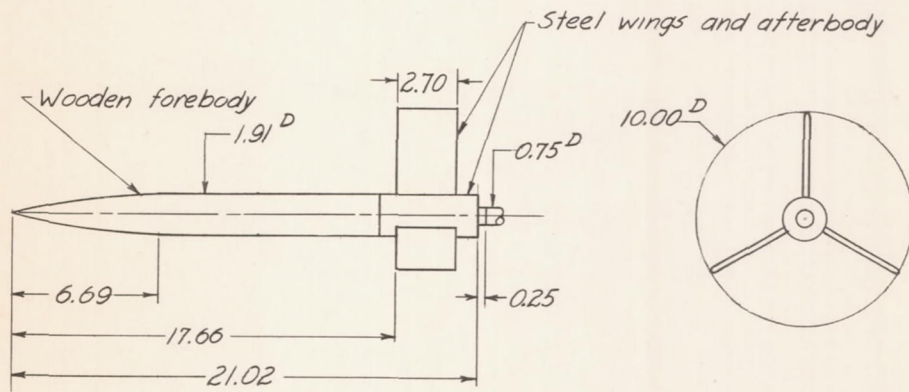


Figure 3.- Sting-mounted test configuration.





Sting-mount test vehicle



Sting-mounted test configuration

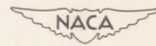


Figure 4.- General arrangement of sting-mount test vehicle. Dimensions are in inches.

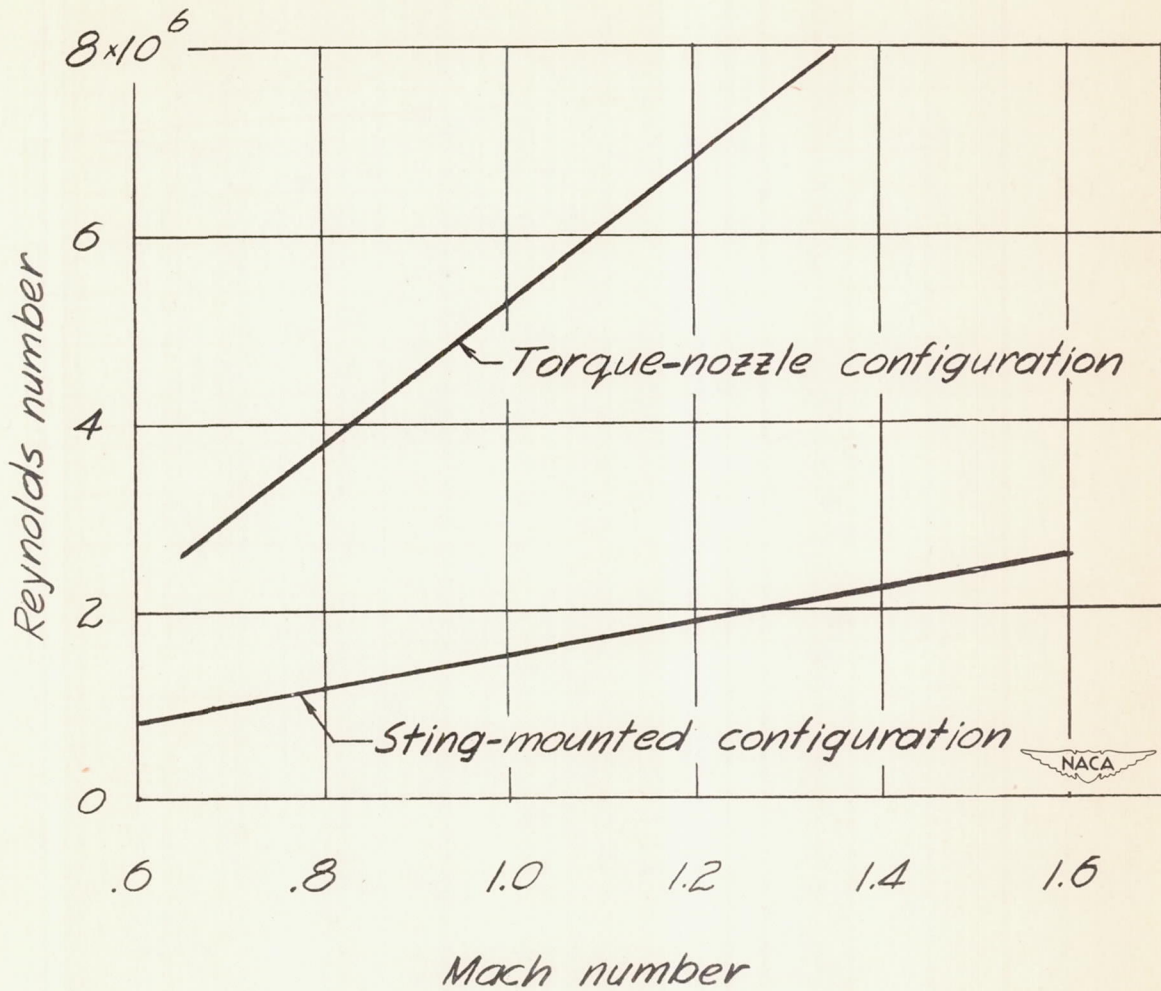
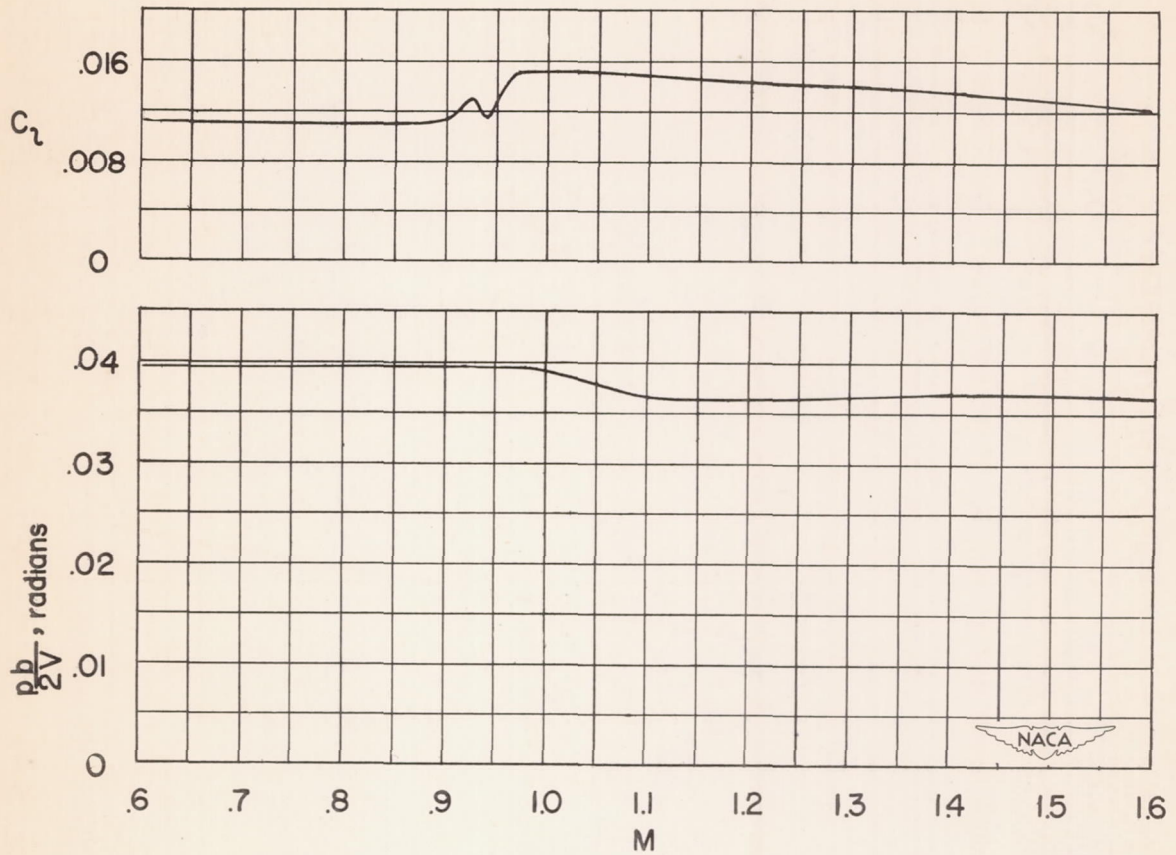
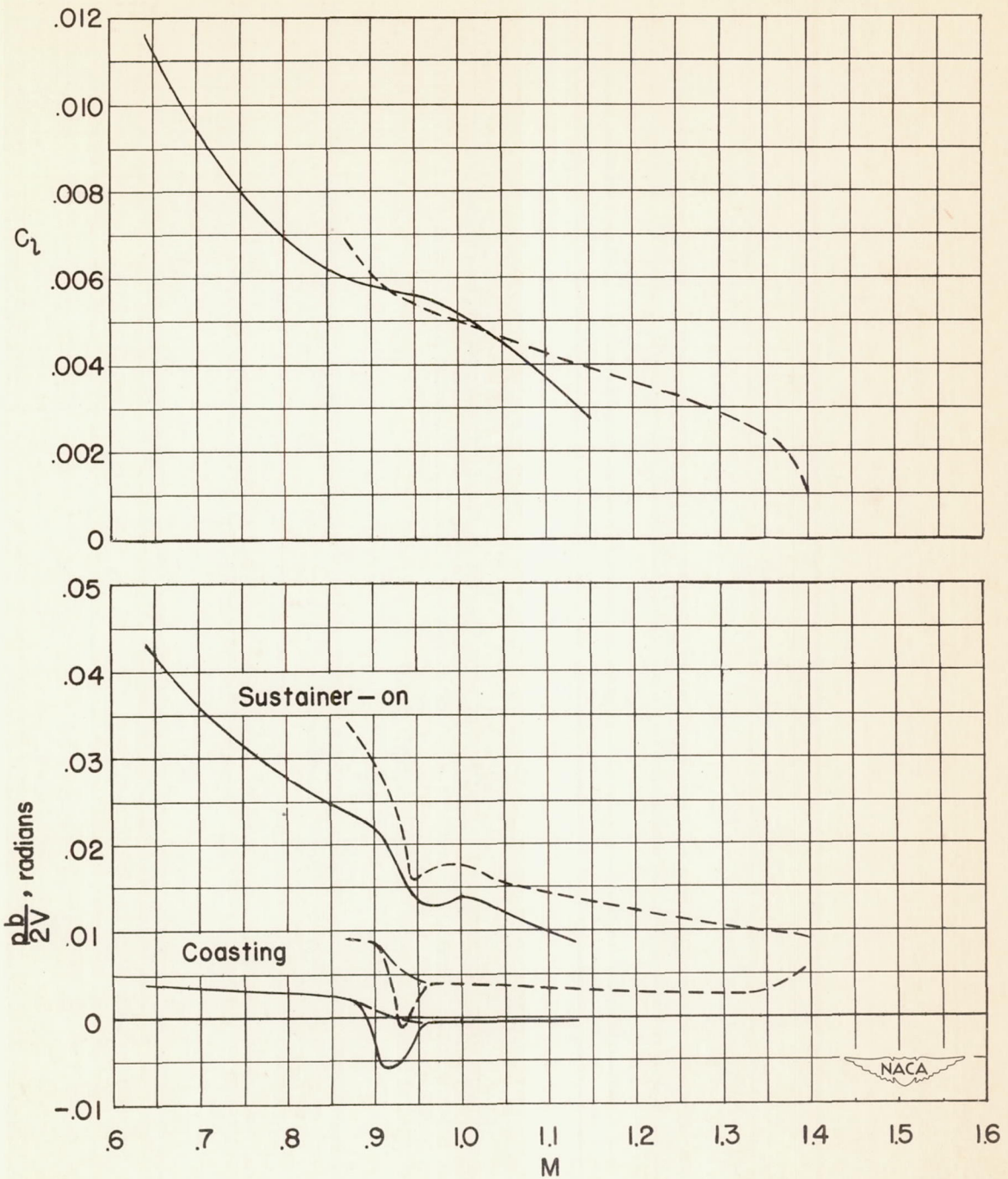


Figure 5.- Variation of Reynolds number with Mach number.



(a) Sting-mount technique.

Figure 6.- Aerodynamic quantities measured by the two testing techniques.



(b) Torque-nozzle technique. Two nominally identical models with different boost rocket motors.

Figure 6.- Concluded.

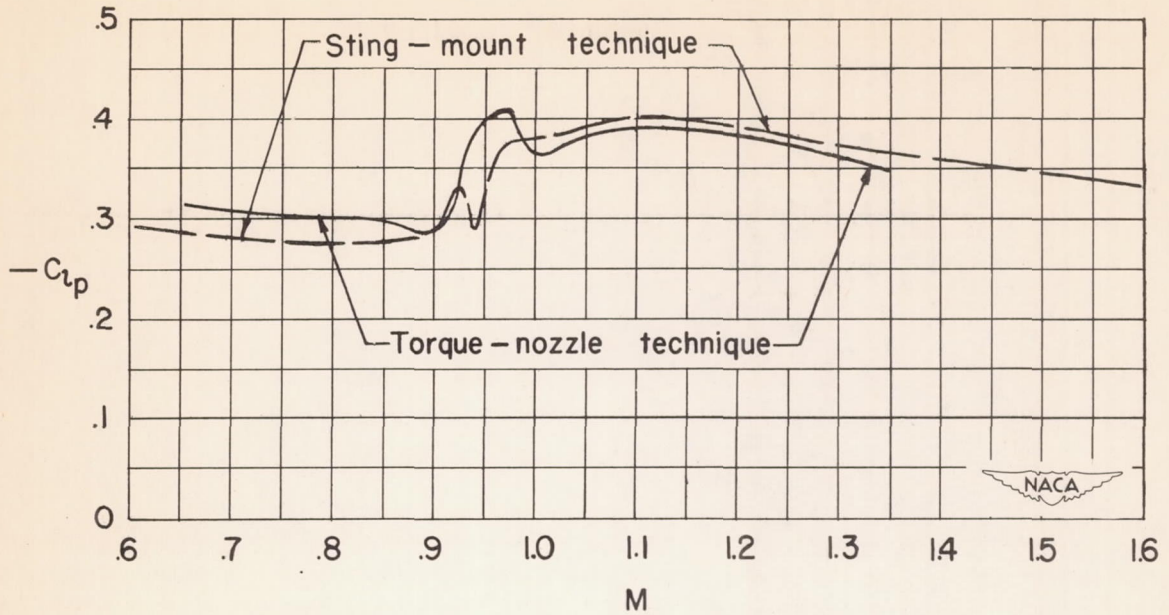


Figure 7.- Comparison damping-in-roll derivative from the sting-mount and torque-nozzle techniques.

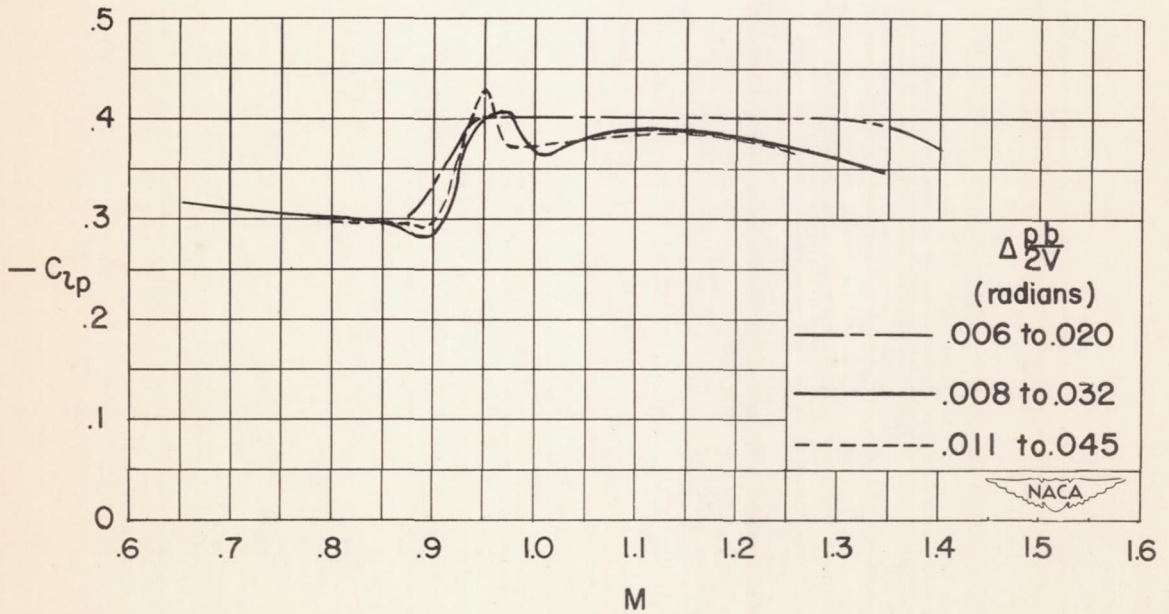


Figure 8.- Variation of C_{lp} values for various ranges of helix angles as determined with the torque-nozzle technique.